Ecology, 103(10), 2022, e3544

Improved inferences about landscape connectivity from spatial capture–recapture by integration of a movement model

Gates Dupont [1,2], Daniel W. Linden [3], and Chris Sutherland [1,4,5]

[1]*Department of Environmental Conservation, University of Massachusetts, 160 Holdsworth Way, Amherst, Massachusetts 01003 USA*
[2]*Organismic and Evolutionary Biology Graduate Program, University of Massachusetts, 204C French Hall, 230 Stockbridge Road, Amherst, Massachusetts 01003 USA*
[3]*Greater Atlantic Regional Fisheries Office, NOAA National Marine Fisheries Service, 55 Great Republic Drive, Gloucester, Massachusetts 01930 USA*
[4]*Centre for Research into Ecological and Environmental Modelling, University of St Andrews, Fife, KY16 9LZ St. Andrews, United Kingdom*

Citation: Dupont, G., D. W. Linden, and C. Sutherland. 2022. Improved inferences about landscape connectivity from spatial capture–recapture by integration of a movement model. Ecology 103(10):e3544. 10.1002/ecy.3544

Abstract. Understanding how broad-scale patterns in animal populations emerge from individual-level processes is an enduring challenge in ecology that requires investigation at multiple scales and perspectives. Complementary to this need for diverse approaches is the recent focus on integrated modeling in statistical ecology. Population-level processes represent the core of spatial capture–recapture (SCR), with many methodological extensions that have been motivated by standing ecological theory and data-integration opportunities. The extent to which these recent advances offer inferential improvements can be limited by the data requirements for quantifying individual-level processes. This is especially true for SCR models that use non-Euclidean distance to relax the restrictive assumption that individual space use is stationary and symmetrical to make inferences about landscape connectivity. To meet the challenges of scale and data quality, we propose integrating an explicit movement model with non-Euclidean SCR for joint estimation of a shared cost parameter between individual and population processes. Here, we define a movement kernel for step selection that uses "ecological distance" instead of Euclidean distance to quantify availability for each movement step in terms of landscape cost. We compare performance of our integrated model to that of existing SCR models using realistic animal movement simulations and data collected on black bears. We demonstrate that an integrated approach offers improvements both in terms of bias and precision in estimating the shared cost parameter over models fit to spatial encounters alone. Simulations suggest these gains were only realized when step lengths were small relative to home range size, and estimates of density were insensitive to whether or not an integrated approach was used. By combining the fine spatiotemporal scale of individual movement processes with the estimation of population density in SCR, integrated approaches such as the one we develop here have the potential to unify the fields of movement, population, and landscape ecology and improve our understanding of landscape connectivity.

Key words: *animal movement; connectivity; cost function; data integration; spatial capture–recapture; Special Feature: Linking Capture–Recapture and Movement.*

Introduction

Current ecological theory frames population processes as emerging from individual behaviors and interactions with local environments that scale up to landscape-level patterns (Levin 1992, Morales et al. 2010, Spiegel et al. 2017). Complementary to this perspective are integrative statistical frameworks for the treatment of data from multiple sources, now a prominent research focus in statistical ecology (Plard et al. 2019). Integrated modeling offers an analytical approach that, by combining data for inference across levels of biological organization, facilitates the advance of ecological theory (McClintock et al. 2021). Spatial capture–recapture (SCR; Efford 2004, Royle and Young 2008) presents an unparalleled opportunity for exploration at the crossroads of these endeavors, built upon an implied model of individual space use related to a model of how individuals are

Manuscript received 16 April 2021; revised 4 June 2021; accepted 15 June 2021. Corresponding Editor: Brett T. McClintock.
[5] Corresponding Author. E-mail: css6@st-andrews.ac.uk

distributed in space. However, the model is typically informed by data on spatially explicit encounter histories that are relatively sparse, if not insufficient, for characterizing more detailed biological processes as opposed to population-level inferences (e.g., spatial variation in density). Data integration can directly address this challenge, providing the ability to improve inferences about mechanism and creating an explicit link between individual-level and population-level processes and landscape-level spatial patterns.

Many methodological extensions of SCR have been motivated by standing ecological theory (see review by Royle et al. 2018), although the extent to which these advances offer inferential improvements is somewhat limited by data requirements. Fortunately, the integration of spatially rich telemetry data into SCR can enable more complexity in the encounter model and improved inferences about density (Royle et al. 2013*c*, Sollmann et al. 2016, Linden et al. 2018), as well as extending the types of spatial encounter data that can be used (Sollmann et al. 2013, Tenan et al. 2017, Murphy et al. 2019). However, much of the focus has been on processing telemetry data to match standard SCR assumptions (e.g., temporal independence of detection locations) and, despite the obvious conceptual linkages, the formal integration of an explicit movement model within SCR is surprisingly rare. Indeed, recognizing and implementing joint movement and SCR models represents the next frontier in spatial population ecology (Royle et al. 2013*b*, McClintock et al. 2021).

Non-Euclidean SCR models relax a restrictive, although statistically convenient, assumption that animal home ranges are stationary and symmetrical (Royle et al. 2013*a*, Sutherland et al. 2015). The implications of this formulation have an even broader impact: the model offers an explicit statistical framework for understanding how landscape structure determines spatial population structure, which is fundamental to a wide range of ecological processes (Tischendorf and Fahrig 2000, Shaw 2020). This is accomplished through the direct estimation of landscape resistance, the mathematical inverse of which represents landscape connectivity, a central feature of all spatially structured populations (Zeller et al. 2012).

Beyond the pervasiveness of structured landscapes, understanding the interplay of landscape connectivity and the emergent spatial population structure at broad spatial scales is especially critical as habitat conversion and fragmentation are increasing globally, with critical implications for the management and conservation of landscapes (Gupta et al. 2019) and for the viability of the majority of extant megafauna (Haddad 2015). However, despite the central role of connectivity in modern conservation science (McRae et al. 2008, Rayfield and Fortin 2011), there remain few methods for empirically estimating its components, let alone simultaneously describing spatial population structure (Tischendorf et al. 2005, Zeller et al. 2012, Hanks and Hooten 2013, Howell et al. 2018). By jointly estimating landscape resistance and population density, the non-Euclidean SCR model directly addresses these challenges using standard ecological encounter history data (Morin et al. 2017, Gupta et al. 2019).

It is perhaps optimistic to expect reliable estimation of cost function parameters using only sparse encounter history data that arise from capture–recapture studies, particularly for elusive, low-density, and wide-ranging species for which estimates of connectivity hold most value (Crooks et al. 2011, 2017, Creel et al. 2020). Small sample sizes of coarse location data limit the space-use complexity in any SCR model, particularly those using non-Euclidean distance, where least-cost paths will have greater uncertainty as the distances in time and space increase between observations. This problem could be mitigated through the integration of fine-scale movement data (e.g., telemetry) and, to accommodate the inevitable temporal autocorrelation, an explicit movement model (Hooten et al. 2017). The integration of explicit movement in the non-Euclidean SCR model should help to inform the direction and strength of cost parameters that are challenging to estimate using SCR data alone (Sutherland et al. 2015).

Here we developed a telemetry-integrated, non-Euclidean SCR model that incorporates an explicit movement model, in which the spatial encounter and telemetry likelihoods share parameters of a cost function. We use a straightforward implementation of a weighted distribution for movement (Johnson et al. 2008) in which non-Euclidean distance defines availability. We evaluated our model using a novel simulation approach that derives spatial encounter and telemetry data from individual-based movement simulations, and analyzed the resulting encounter histories using our integrated SCR–movement cost models, with standard SCR models used for benchmarking. We evaluated the performance of the model under a range of conditions designed to test sensitivity to data quality and the number of telemetered individuals. As a case study, we applied the model to data on an American black bear (*Ursus americanus*) population (Sun 2014) and discuss these results in the context of the simulations.

Methods

Spatial capture–recapture with non-Euclidean distance

We begin with a brief description of a standard, constant-density SCR model with a binomial encounter model. Specifically, we have spatially indexed encounters y_{ij} representing the number of detections of individual i at detector j across K surveys. With no survey-specific variation, we model the encounters as binomial random variables having an encounter probability p_{ij} conditional on the latent activity center $\mathbf{s}_i$:

$$y_{ij}|\mathbf{s}_i \sim \text{Binomial}\left(K, p_{ij}\right).$$

We assume a homogeneous point process for $\mathbf{s}_i$ across the support of the state space $\mathcal{M}$ which will require integration during likelihood estimation. Encounter probability is a decreasing function of the Euclidean distance $d_{\text{Euc}}(\mathbf{x}_j, \mathbf{s}_i)$ between the activity center $\mathbf{s}_i$ and detector $\mathbf{x}_j$:

$$p_{ij} = p_0 \times \exp\left(-\frac{d_{\text{Euc}}(\mathbf{x}_j, \mathbf{s}_i)^2}{2\sigma_{\text{det}}^2}\right),$$

where p_0 is the baseline encounter probability and σ_{det} is the scale parameter of a Gaussian kernel (i.e., the half-normal detection function), both of which are parameters to be estimated. We refer to this model as M_{Euc}.

The encounter function of M_{Euc} is assumed to be proportional to the individual's home range, which implies that home ranges are stationary and symmetric. While statistically convenient, this core assumption is unlikely to hold in reality. Royle et al. (2013*a*) demonstrated how the Euclidean distance assumption can be relaxed with direct estimation of the parameter of a cost function by modeling encounter probabilities using estimated distances of least-cost paths, $d_{\text{lcp}}(\mathbf{x}_j, \mathbf{s}_i)$, rather than simple measures in Euclidean space. This distance substitution gives rise to a model that we refer to as M_{lcp}, where:

$$p_{ij} = p_0 \times \exp\left(-\frac{d_{\text{lcp}}(\mathbf{x}_j, \mathbf{s}_i)^2}{2\sigma_{\text{det}}^2}\right).$$

The cost distance is calculated as follows. First consider a discrete landscape $\mathcal{V}$ of some predefined resolution, where each pixel ν has associated coordinates $\mathbf{x}$ and a covariate value, $z(\nu)$. Any path P between two locations (e.g., $\mathbf{x}$ and $\mathbf{x}'$) consists of M transitions between pairwise adjacent pixels $\{\boldsymbol{\nu}_0, \boldsymbol{\nu}_1, \ldots, \boldsymbol{\nu}_M\}$ and we define a cost function for moving from pixel to pixel as:

$$\text{cost}(\boldsymbol{\nu}_m, \boldsymbol{\nu}_{m+1}) = \frac{\exp(\alpha_1 z(\boldsymbol{\nu}_m)) + \exp(\alpha_1 z(\boldsymbol{\nu}_{m+1}))}{2}$$

Here, α_1 is a cost parameter to be estimated. For a given value of α_1 and all L reasonable paths, the least-cost path d_{lcp}, calculated using Dijkstra's Algorithm (Dijkstra, 1959), is:

$$d_{\text{lcp}}(\mathbf{x}, \mathbf{x}') = \min_{P_1, \ldots, P_L} \sum_{m=0}^{M_L} \text{cost}(\boldsymbol{\nu}_m, \boldsymbol{\nu}_{m+1}) \times d_{\text{Euc}}(\boldsymbol{\nu}_m, \boldsymbol{\nu}_{m+1}).$$

Conceptually, the cost surface is a functional transformation of a spatially varying covariate surface using α_1. When $\alpha_1 = 0$, $d_{\text{lcp}}(\mathbf{x}_j, \mathbf{s}_i) = d_{\text{euc}}(\mathbf{x}_j, \mathbf{s}_i)$, and as α_1 increases, cost distance diverges from Euclidean distance. When informed by spatially structured individual encounter data, this divergence of distance metrics provides a mechanism for estimating α_1, i.e., finding the value of the cost parameter that best describes the spatial pattern of the encounter history data.

Regardless of the encounter function used, the latent activity centers must be integrated out of the joint likelihood (over the support of $\mathcal{M}$) to form the marginal likelihood of the encounter data, $[\mathbf{y}|\alpha_1, p_0, \sigma_{\text{det}}]$. Following Borchers and Efford (2008) we assumed that population size is a Poisson random variable such that the joint likelihood can enable direct estimation of density as the mean intensity, λ, of a Poisson point process:

$$\mathcal{L}_{\text{SCR}}(\alpha_1, p_0, \sigma_{\text{det}}, \lambda|\mathbf{y}) = \left\{\prod_{i=1}^{n} [\mathbf{y}_i|\alpha_1, p_0, \sigma_{\text{det}}]\right\} \Lambda^n \exp(-\Lambda(1-\pi_0))$$

where $\Lambda = \lambda||\mathcal{M}|| = E(N)$ and π_0 is the probability of an all-zero capture history.

Animal movement with non-Euclidean distance

Here we describe a simple approximation of a spatiotemporal point process model for movement (Hooten et al. 2017) where the probability of an observed location is determined by a redistribution kernel (Moorcroft and Barnett 2008) conditional on the previous location (i.e., a first-order Markov process) and an attraction to the home range center. This type of weighted distribution approach allows for estimation of resource selection from telemetry (Christ et al. 2008, Johnson et al. 2008) although our model has reduced complexity and focuses on the availability in terms of cost distance. Critically, it is the cost parameter α_1 that is to be estimated from a collection of telemetry locations.

Consider an observed movement trajectory for individual i over T fixed-interval time steps, $\boldsymbol{\mu}_{it} = \boldsymbol{\mu}_{i1}$, $\boldsymbol{\mu}_{i2}, \ldots, \boldsymbol{\mu}_{iT}$, where we assume there is no observation error in the observed location (i.e., $u \equiv \mu$). To model movement between steps we define an availability function or redistribution kernel, $k(\boldsymbol{\mu}_{it}|\boldsymbol{\mu}_{i,t-1}, \theta)$, where the relative probability of a location $\boldsymbol{\mu}_{it}$ is a decreasing function of both the cost distance from the previous location $\boldsymbol{\mu}_{i,t-1}$ and the cost distance from the average of all locations $\overline{\boldsymbol{\mu}}_i$ for individual i:

$$k(\boldsymbol{\mu}_{it}|\boldsymbol{\mu}_{i,t-1}, \theta) = t = \exp\left(-\frac{d_{\text{lcp}}(\boldsymbol{\mu}_{it}, \boldsymbol{\mu}_{i,t-1})^2}{2\sigma_{\text{step}}^2} - \frac{d_{\text{lcp}}(\boldsymbol{\mu}_{it}, \overline{\boldsymbol{\mu}}_i)^2}{2\sigma_{\text{home}}^2}\right).$$

The location $\overline{\boldsymbol{\mu}}_i$ is treated as known and is used to capture the effect of central tendency in movement (in this case, within the home range). Spatial scale parameters

represent the variance in movement between observed locations in the movement trajectory (σ_{step}) and across the home range (σ_{home}). We note also that σ_{home} differs from σ_{det} from the SCR model in that there is not an additional detection process occurring for telemetry data as there is for SCR data. Based on this redistribution kernel, the normalized conditional probability of the observed locations becomes:

$$\left[\boldsymbol{\mu}_{it}|\boldsymbol{\mu}_{i,t-1},\theta\right]=\frac{k(\boldsymbol{\mu}_{it}|\boldsymbol{\mu}_{i,t-1},\theta)}{\int k(\boldsymbol{\mu}|\boldsymbol{\mu}_{i,t-1},\theta)d\boldsymbol{\mu}}$$

For our discrete landscape from earlier, the locations $\boldsymbol{\mu}$ are associated with pixels $\boldsymbol{\nu}$ and the integral in the denominator above becomes a summation across all $\boldsymbol{\nu}\in\mathcal{V}$:

$$[\nu_{it}|\nu_{i,t-1},\theta]=\frac{k(\nu_{it}|\nu_{i,t-1},\theta)}{\sum_{g=1}^{\mathcal{V}}k(\nu_g|\nu_{i,t-1},\theta)}$$

To accommodate an excess number of steps where pixel location does not change, potentially representing a behavioral state resulting in no movement, we model the probability $\Pr(\nu_{it}\neq\nu_{i,t-1})=\psi$ that an individual moves from the last known location/pixel. The likelihood for the movement model therefore has the following form:

$$\mathcal{L}_{\text{move}}(\alpha_1,\sigma_{\text{step}},\sigma_{\text{home}},\psi;\boldsymbol{\nu})=\prod_{i=1}^{N_{\text{tel}}}\prod_{t=2}^{T}\psi\left(\frac{k(\nu_{it}|\nu_{i,t-1},\theta)}{\sum_{g=1}^{\mathcal{V}^*}k(\nu_g|\nu_{i,t-1},\theta)}\right)^{I\left(\nu_{it}\neq\nu_{i,t-1}\right)}\times(1-\psi)^{I\left(\nu_{it}=\nu_{i,t-1}\right)}$$

Here, the denominator calculates availability for pixels $\nu_g\in\mathcal{V}^*$, representing all pixels in the discrete landscape not including $\nu_{i,t-1}$. Note, we do not model the first location ($t=1$) under the assumption that this loss of information is small with a long time series of telemetry locations (Johnson et al. 2008), although the first location could be modeled as: $\mu_{i1}:\text{Normal}(\bar{\mu}_i,\sigma_{\text{home}})$, in discrete space.

Integrating the movement model into SCR

The joint SCR–movement likelihood combines the cost-based SCR likelihood and cost-based movement likelihood through shared estimation of the cost parameter α_1. We refer to this model as iM_{lcp}, where "*i*" stands for *integrated*:

$$\mathcal{L}_{iM_{\text{lcp}}}(\alpha_1,p_0,\sigma_{\text{det}},\lambda,\sigma_{\text{step}},\sigma_{\text{home}},\psi;\mathbf{y},\boldsymbol{\nu})=\mathcal{L}_{\text{SCR}}\times\mathcal{L}_{\text{move}}.$$

Note that the joint estimation of cost assumes that the effect of landscape resistance is equivalent across scales of movement, whether steps between telemetry locations or the long-term utilization of a home range resulting in trap encounters. An assumption of consistency should be reasonable as cost paths are scaled by distance and calculated as accumulations of pixels with the same resolution.

The joint likelihood treats data from spatial encounter histories and telemetry as independent, i.e., there is no overlap in identities of passively detected and telemetered individuals. Although this is not always the case in practice, it does create flexibility in the model to allow for sampling from different time periods, and importantly, should have little consequence on the primary biological inference objectives, namely: cost and density (Royle et al. 2013*c*). The joint likelihood function is provided in Data S1. Model parameters are estimated using maximum likelihood methods (Borchers and Efford 2008) in `R` (R Core Team 2020). Least-cost paths are computed using Dijkstra's Algorithm (Dijkstra et al. 1959) implemented in the `R` package `gdistance` (Etten 2017).

Evaluation by simulation

Our primary evaluations of the model were conducted through simulation, testing sensitivity to data quality and comparing performance against the standard Euclidean and non-Euclidean SCR-only models.

We began by defining the SCR state space ($\mathcal{M}$), which is the area within which all individual activity centers are simulated and the area for which density is estimated. We defined a grid of 25×25 points representing the centers of 1×1 unit pixels. Activity centers can be located at any pixel within $\mathcal{M}$, but to allow unconstrained movement trajectories, especially for those activity centers located close to the edges, we defined a second landscape, $\mathcal{V}$, comprising all theoretically possible movement trajectories given our simulation settings, such that $||\mathcal{V}||>||\mathcal{M}||$. We defined $\mathcal{V}$ as a grid of 137×137 points representing the centers of each 0.25 unit $\times$ 0.25 unit pixels in the movement landscape, noting that the resolution of $\mathcal{V}$ is finer than $\mathcal{M}$ to allow finer scale movement trajectories that better approximate continuous space. We generated a cost covariate landscape by assigning pixel values in $\mathcal{V}$ generated under a Gaussian random field model with weak autocorrelation (maximum autocorrelation range = 6 pixels), which was then scaled from 0 to 1 (Fig. 1a). Gaussian random fields were generated in `R` using the package `NLMR` (Sciaini et al. 2018).

We simulated movement trajectories and subsequently derived encounter data as emergent properties of the movement data based on proximity to an array of traps. To do so, we randomly generated $N=100$ activity centers, with replacement, from $\mathcal{M}$. Then, using the model described above and the availability landscape $\mathcal{V}$, we simulated movement tracks for every individual using the activity center as the initial location. Movement paths were generated for $T=2160$ times steps (or "fixes") approximating hourly fixes over a hypothetical three-month period (Fig. 1b). Parameters of the data-

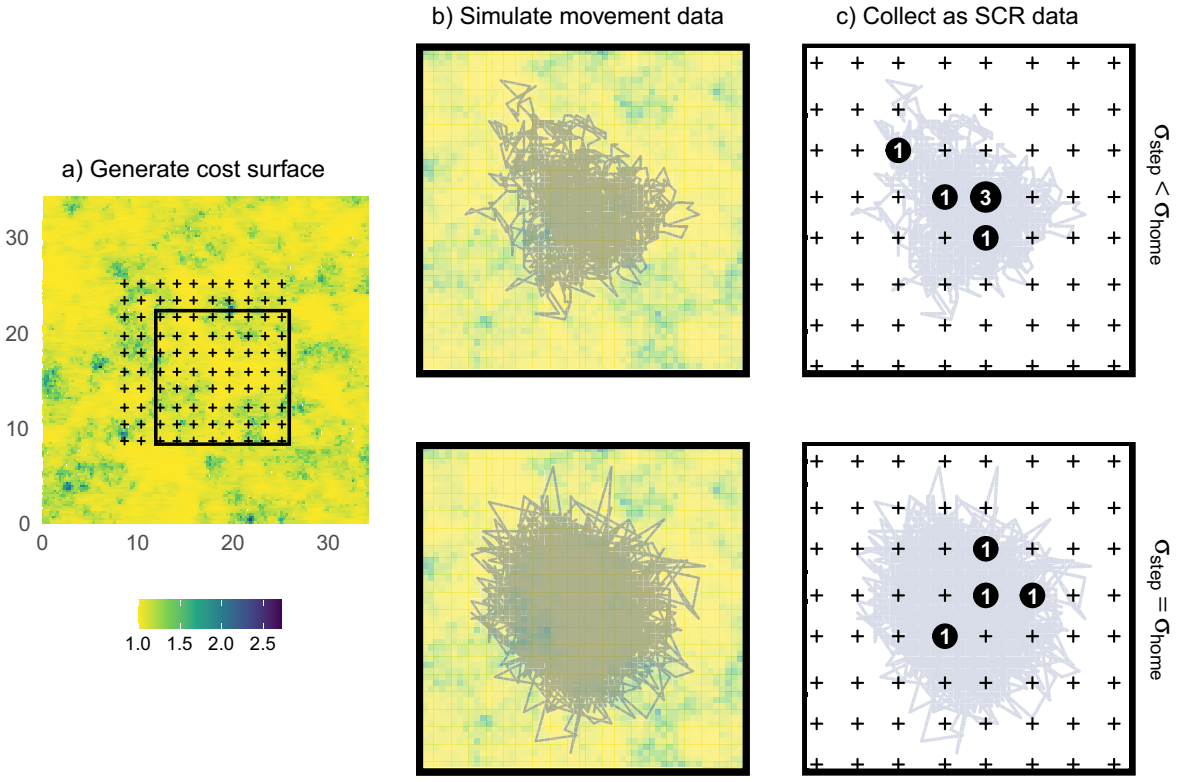

FIG. 1. General outline of realistic movement simulations, with parts (a–c) representing consecutive steps in the workflow. (a) First, using a Gaussian field model we generate a cost surface, where yellow is low cost and dark purple is high cost. Proximity detectors (traps) are black crosses, and the black bounding box indicates the inset region shown in (b) and (c). (b) Activity centers are generated randomly (not shown) and are used to simulate movement tracks, shown in grey. These tracks differ in the value of σ_{step}, either small (top) or large (bottom), and relative to σ_{home} as shown on the right side. (c) Movement tracks are thinned and recorded as trap captures, collected as SCR data, as shown by the black circles with white text for the number of captures at that trap.

generating movement model were chosen to reflect biologically realistic parameter combinations and are provided in Table 1.

Spatial encounter histories were then derived from the simulated movement paths based on a 10×10 trapping grid located in the center of the study area (Fig. 1c). If a movement step contained a trap, it was 'detected' with probability 0.1, where the binomial thinning ensures that the distribution of recaptures and spatial recaptures were realistic when compared with empirical SCR data (see Appendix S1: Fig. S1 for scenario-specific summaries of the spatial encounter histories). Per standard design recommendations (Dupont et al. 2021b), detectors were spaced 1.75 units apart (approx. $2\sigma_{home}$) leaving a three unit ($3\sigma_{home}$) buffer to the edge of $\mathcal{M}$.

This approach of deriving spatial encounter histories from individual movement data differs from the traditional approach of simulating data directly from the SCR model. We believe our approach provides a valuable simulation framework for exploring SCR model performance and sensitivity under a range of potential assumption violations and, as demonstrated here, movement characteristics.

We were interested in exploring model performance as a function of two features of telemetry data: the number of telemetered individuals used in the analysis, and ratio of the spatial variance parameters. First, to evaluate whether the performance of the integrated model was sensitive to the number of telemetered individuals included, we considered the inclusion of one, three, and five individuals. Second, we evaluated model performance with respect to the variance ratios, which we motivate conceptually as representing potential differences in either species propensity for movement or the telemetry fix rate. Specifically, we tested two ratios: the spatial scale of the steps σ_{step} being one-quarter that of the home range space-use parameter σ_{home} (the "small-σ_{step} scenario," $\sigma_{step} = 0.25\sigma_{home}$), and a "large-$\sigma_{step}$ scenario" where the ratio was 1 ($\sigma_{step} = \sigma_{home}$).

We simulated 100 data sets under each σ_{step}-ratio scenario. For each, the activity centers, corresponding movement paths (i.e., telemetry data), and the cost surface were generated randomly. Individuals were subject to detection via the trapping array resulting in n individuals with non-zero encounter histories (i.e., SCR data). We analyzed the SCR and telemetry data using the

TABLE 1. Parameters of the integrated model along with predefined values used for the simulation study, where parameter name, symbol, and biological interpretation are shown in each row.

Parameter	Symbol	Small-σ_{step}	Large-σ_{step}	Biology
Cost	α_1	1	1	Resistance of the landscape to movement
Baseline detection	p_0	–	–	Detection probability at the activity center in the home range
Detection spatial scale	σ_{det}	2.5	2.5	Scaling factor determining size of the detection kernel
Home range spatial scale	σ_{home}	2.5	2.5	Scaling factor determining size of the home range
Density	λ	0.16	0.16	Number of individuals in the state space
Step distance spatial scale	σ_{step}	**0.625**	**2.5**	Scaling factor determining the size of the movement kernel
Probability moved	ψ	0.9	0.9	The probability that an individual moves, i.e., that it leaves the pixel

Note: Numbers in bold highlight the main difference between the two simulation scenarios, small-σ_{step} and large-σ_{step}.

integrated non-Euclidean model where the one, three, or five movement tracks were randomly selected from all 100 individuals. As a comparison, we also analyzed each data set without telemetry data, i.e., an SCR-only data set, using the non-Euclidean SCR model (M_{lcp}), which is a special case with 0 telemetered individuals. In summary, we fitted two SCR variants—not integrated and integrated—to each data set, and for the integrated model consider one, three, and five telemetered individuals, i.e., four comparisons for each σ_{step}-ratio scenario. We note that, rather than model the detections as a function of the spatiotemporal proximity to the movement path as per the data-generating procedure, SCR detections are modeled as a function of distance to the latent activity center. The former requires an additional conditional structure and individuals that appear in both the telemetry and SCR data. While dependency is straightforward (e.g., Linden et al. 2018) a latent movement model for the encounter data would be a computationally intensive extension for our model, which we do not consider.

For the eight simulation sets, we evaluated model performance by computing percent relative bias for each parameter. For model M_{lcp} in the large-σ_{step} scenario, we removed four simulation results due to poor model fit. All simulations and analyses were conducted in R version 4.0.3 (R Core Team 2020), and are available in our Open Science Framework repository (Dupont et al. 2021a).

Case study: New York black bears

As a demonstration of the model in practice and its relative performance, we analyzed data from a study of black bears in western New York (Sun 2014). The data consist of 103 hair snares from a non-invasive genetic mark–recapture study, which resulted in spatial encounter histories for 33 individuals. In addition to the trapping, three bears were fitted with GPS collars in the same study area during the same time period (Fig. 3a). These data are described in detail in Sun (2014).

We used percent forest ("% forest") as the cost covariate, but note that our model can easily accommodate the simultaneous estimation of multiple cost parameters associated with multiple landscapes. We derived % forest from the National Land Cover Database (NLCD) (Yang 2018) by aggregating the 30-m raster to a 500 m resolution and calculating the proportion of forest pixels therein (Fig. 3a). NLCD data were accessed using the R package FedData (Bocinsky 2016). We defined the state space as a 4,968 km^2 rectangular area with a $3\sigma_{det}$ buffer around the trapping array, based on the σ_{det} estimated in previous analyses of these data (Royle et al. 2013*c*, Morin et al. 2017), and a resolution approximating σ_{step}, calculated from the raw fix locations using Euclidean distance.

We analyzed the bear data using the four models described above (see also: Appendix S1: Table S1). Our primary comparison was between the existing model M_{lcp} and our integrated model, iM_{lcp}. For more thorough reference and comparison, we included all applicable null models. To explore the effect of individual variation, we also fitted the integrated model including only a single individual at a time. These analyses were conducted in R and all code is provided in our Open Science Framework repository (Dupont et al. 2021a).

After obtaining model results, we followed the procedure of Morin et al. (2017) to produce surfaces of realized density (i.e., the estimated density of activity centers conditional on the observed data) and density-weighted connectivity (i.e., expected pixel use based on estimated cost and weighted by realized density).

RESULTS

Evaluation by simulation

We first report results from the small-σ_{step} scenario. The standard non-Euclidean SCR model (M_{lcp}) produced a biased estimate of cost (%RB = −17) with relatively low precision (Fig. 2; Appendix S1: Table S2). In contrast, and consistent with the marked robustness of SCR, estimates of density were unbiased (Fig. 2). In terms of estimating the cost parameter, integrating telemetry data improved performance considerably: data from a single individual alone reduced the bias to just

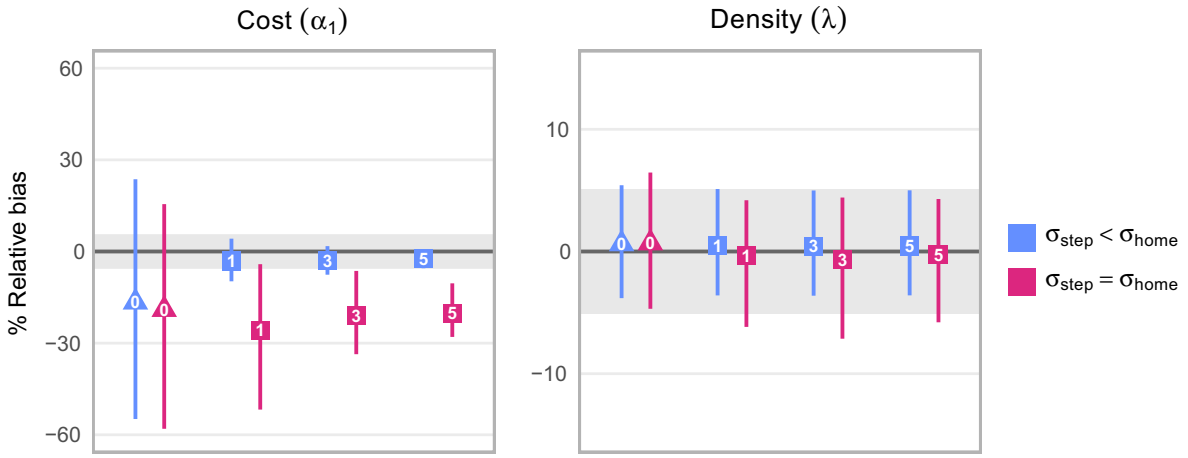

FIG. 2. Percent relative bias from simulation results. To illustrate estimator precision, vertical lines are 50% confidence intervals. Here, 50% intervals are proportional to 95% intervals but offer a visual balance of bias and associated variance. Blue and fuschia shapes represent the small- and large-σ_{step} scenarios, respectively. Triangles represent model M_{lcp} and squares represent model iM_{lcp}, with an increasing number of telemetered individuals (inset number). Gray shaded areas show an acceptable amount of bias (±5%). Full results are given in Appendix S1: Table S2.

−3% and markedly improved the precision (Fig. 2; Appendix S1: Table S2). Telemetry data from more individuals resulted in further improvements (Fig. 2; Appendix S1: Table S2).

Thus, the integrated model consistently produced unbiased and precise estimates of both the data-generating movement parameters and density (Fig. 2; Appendix S1: Table S2). Moreover, the performance (both bias and precision) improved with the addition of more telemetered individuals (Fig. 2; Appendix S1: Table S2).

In the large-σ_{step} scenario, and consistent with the small-σ_{step} scenario, estimates of density were unbiased irrespective of whether integration was used, although precision was marginally poorer (Fig. 2). What was strikingly different in the large-σ_{step} scenario, where distances between locations were larger, and therefore number of possible least-cost paths was greater, was the inability to reliably estimate the cost parameter. In all cases, regardless of number of telemetered individuals included, the integrated model produced biased estimates of α_1, ranging from −26% to −20% (Fig. 2; Appendix S1: Table S2).

Case study: New York black bears

The results from the black bears case study were consistent with the simulation results suggesting no appreciable influence of cost or telemetry integration on density estimates (Table 2). Most importantly in the context of this study, the integrated model (iM_{lcp}) captured an effect of cost that was both stronger and more precise (estimate: −1.17 [SE: 0.11] vs 0.23 [SE: 0.75]; Table 2) than the SCR-only model (M_{lcp}). In fact, the standard model suggested no compelling evidence of a resistance effect due to forest, whereas the integrated model reveals a strong and highly plausible negative effect of decreased resistance as forest cover increases.

Finally, fitting the integrated model to each of the three individuals separately indicated some heterogeneity

TABLE 2. Results from American black bears analysis.

Model	α_1	log(λ)	σ_{det}	p_0	ψ	σ_{step}	σ_{home}	−loglik	AIC
M_{Euc}	–	−3.843	1.238	−2.768	–	–	–	124.32	254.64
	–	(0.254)	(0.139)	(0.361)	–	–	–		
M_{lcp}	0.226	−3.845	1.284	−2.736	–	–	–	124.27	256.54
	(0.753)	(0.254)	(0.209)	(0.377)	–	–	–		
iM_{Euc}	–	−3.843	1.238	−2.768	−0.666	−0.195	1.914	3,874.45	7,762.90
	–	(0.254)	(0.139)	(0.361)	(0.048)	(0.020)	(0.164)		
iM_{lcp}	−1.172	−3.841	0.812	−2.882	−0.666	−0.624	1.439	3,835.42	7,684.84
	(0.111)	(0.255)	(0.138)	(0.368)	(0.048)	(0.044)	(0.165)		

Note: From left to right: fitted model (see *Methods: Case study for reference*), all estimated parameters showing point estimates with standard errors directly below in parentheses, and the negative likelihood value.

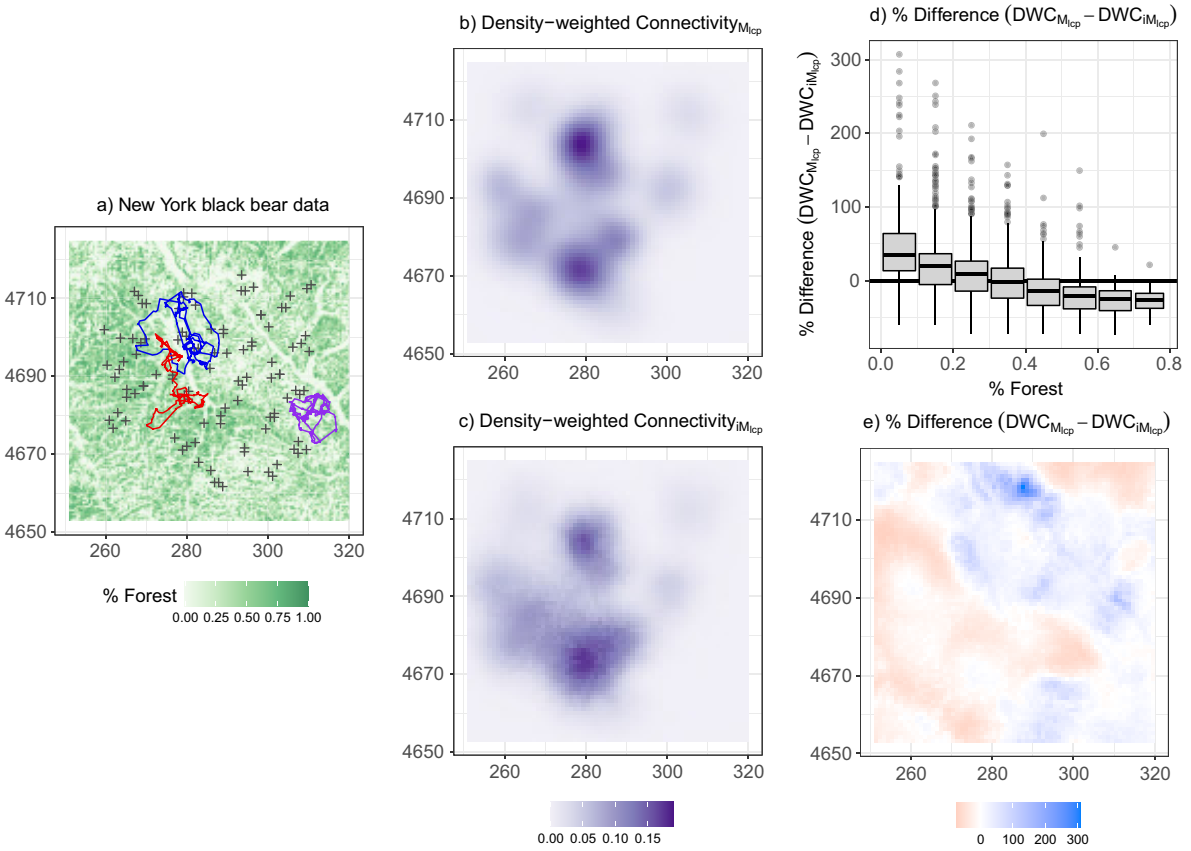

FIG. 3. Black bear data and results. (a) The % forest covariate surface, black crosses are hair snares and colored paths are movement tracks for three individuals. Density-weighted connectivity (DWC) from model M_{lcp} (b), and from model iM_{lcp} (c). Boxplot representation of the percent difference between DWC from model M_{lcp} and model iM_{lcp} (d). Finally, (e) is a spatial representation of the percent DWC differences (i.e., c minus d).

in the estimated cost parameter, but consistency in the direction and relative magnitude of the effects (Appendix S1: Fig. S2).

DISCUSSION

Integrated data modeling represents a promising statistical framework for testing and advancing theory about ecological processes across multiple scales. Here, we illustrated an integration of trap encounters and telemetry locations that embedded an explicit movement model within spatial capture–recapture, leveraging their conceptual linkages. Together, movement data provide high-resolution information on step selection, and encounter history data allow for landscape-scale inference about spatial patterns of density, facilitating an improved understanding of how landscape-scale patterns of density and connectivity emerge from individual-level processes. Specifically, we provide an intuitive and flexible statistical framework for integrating telemetry and encounter history data; we highlight the value of an integrated modeling approach for improved inferences about the processes of density, space use, and landscape connectivity simultaneously.

Our method for integrating fine-scale telemetry data offers key performance improvements over the original non-Euclidean SCR model, and suggests that these improvements are related to the quantity and quality of the telemetry data. Here we considered including data on only a few individuals (one, three, five), and observed precision gains for the cost parameter that increased with the number of telemetered individuals added. In contrast, estimates of density did not benefit from the integration, possibly due to the lack of spatial variation in density (e.g., Linden et al. 2018). Notably, performance improvements were only realized in scenarios where the spatial scale of consecutive fixes is much less than the spatial scale of individual space use; here, the integrated model is both unbiased and more precise than the non-integrated version. When the distance between fixes is relatively large, there is a loss of precision in both density and cost, and estimates of cost are negatively biased. The latter is likely to be due to uncertainty about the exact path taken between two locations at larger distances, which degrades

the effect size of any cost relationships. In practice, the movement integrated model is recommended when telemetry data are available, motivated by both the conceptual and empirical advantages presented here, but we note that efforts should be made to select fix rates that result in short step lengths relative to the size of the home range (i.e., $\sigma_{step} < \sigma_{home}$). In general, and when individual heterogeneity in movement is low, fix rate appears to be more important than the number of collared individuals in terms of estimator improvements.

It is perhaps optimistic to expect accurate inference about fine-scale movement processes from coarse-scale SCR data (Sutherland et al. 2015). Indeed, this was evident from both the simulations and the bear case study, where cost parameters are not well estimated without the integration of high-resolution telemetry data via an explicit movement model. The addition of even a single telemetered individual resulted in the recovery of the cost parameters with accuracy and precision, a pattern noted in the context of SCR models that integrate resource selection functions (Royle et al. 2013*c*). Although it is not advisable to rely on a single animal for inferences due to individual heterogeneity in movement (Revilla and Wiegand 2008), the bear case study did indicate consistency across individuals in the direction and magnitude of the cost estimate (Appendix S1: Fig. S2). Either way, the benefits of the non-Euclidean model may only be realized with large amounts of spatial recaptures (which is unlikely in practice), or through integrated approaches such as we develop here. Estimation of landscape connectivity is an important endeavor in wildlife conservation, yet is not well developed, especially using empirical observations (Zeller et al. 2012). Our integrated model provides an important formal statistical link between individual data and estimates of landscape connectivity (Fig. 3).

We demonstrated clear improvements in SCR model performance with telemetry integration, as has been shown previously (Royle et al. 2013*c*, Sollmann et al. 2013, Linden et al. 2018). These other approaches formalized telemetry integration by joint estimation of shared parameters, particularly the detection scale parameter (see our exploration on sharing the space-use parameter within this model presented in Appendix S2). Royle et al. (2013*c*) additionally relied on diluting or thinning their high-resolution telemetry data to match the coarser scale of spatial encounter histories rather than integrating an explicit movement model. Although thinning telemetry data removes autocorrelation to satisfy independence assumptions, it removes by definition the conditional dependence in the observed locations that directly reflects fine-scale decisions about movement. Retaining the sequential structure of movement paths by explicitly modeling those decision processes yields improved insights about animal movement (McClintock et al. 2021). By also leveraging the less obvious connection between SCR and movement models, namely the existence of a shared cost function, we allowed those benefits to be realized at the population and landscape level.

In contrast with conventional SCR simulation approaches, in which encounter history data are simulated from the expected encounter model, we allowed encounter data to emerge as a property of simulated animal movement paths. We did not fit this data-generating model (due to the additional computational complexity), but used it for simulation as it offers some specific benefits. Movement paths are allowed to evolve from a wide range of well established and flexible models that can be parameterized according to known species characteristics (Hooten et al. 2017). As a result, the emergent encounter data arise as a property of the movement model rather than the specified SCR model, arguably a more preferable challenge for model evaluation with greater ecological realism. This provides a flexible simulation structure for better understanding how model performance varies under a wider range of scenarios that includes considerations specific to the system, the species, or sampling. For example, we investigated model performance for two scenarios related to the ratio of the variance parameters σ_{step} and σ_{home}, which we motivated as being representative of potential differences in either species propensity for movement or the telemetry fix rate, but ultimately that give rise to different data structures (Fig. 1b). In terms of density estimation, these differences had little effect, apart from a marginal increase in precision. However, the models were sensitive to the characteristics of the data when estimating parameters related to movement. In the large ratio scenario, estimates of the cost parameter (α_1, Fig. 2) and the movement scale parameter (σ_{step}; Appendix S1: Table S2) were systematically biased low, whereas the estimated SCR spatial scale parameter (σ_{det}) was always higher (Appendix S1: Table S2).

Our simulation structure also allowed us to consider the consequences of incorrect parameter sharing, motivated by the high prevalence in the SCR literature of interpreting σ_{det} as an estimate of space use, rather than explicitly defining it as a detection range which is *proportional to* space use. Under this interpretation, there is likely to be a temptation to assume some equivalency (i.e, $\sigma_{det} = \sigma_{home}$), which we show produces negatively biased estimates of cost and density (Appendix S2). Depending on the assumed model of individual movement, the variance of a bivariate normal kernel estimated from the location data may not be equivalent to that as estimated by the encounter histories using SCR. Ultimately, our simulations highlight that strict biological interpretations of movement parameters from standard SCR models should generally be avoided.

Our movement model addresses a fraction of what is possible among the diverse and complex animal movement processes for which models have been developed (Hooten et al. 2017). Our implementation of the weighted distribution approach makes a restrictive assumption that telemetry fixes have regular time

intervals and, while it did not affect simulations, it did probably affect the black bear case study. We expect that the consequence was similar to that for spatial encounter data alone, namely that landscape cost was slightly underestimated when hourly steps were diluted by steps with longer time periods between. This problem could be explored through simulation or addressed more comprehensively by the movement model likelihood (Johnson et al. 2008). Relatedly, the first-order Markov relationship between steps ignores the history of movements prior to the step in time $t - 1$, and this covariance across time could be estimated (Johnson et al. 2008). Finally, we did not model the latent movement of individuals from the encounter data (i.e., the data-generating model), which could inform far more spatial and temporal complexity in the encounter model at the expense of computational burdens. Our approach was intended to illustrate the clear benefits of including a straightforward movement model when integrating telemetry into SCR using a likelihood approach that can be easily implemented by extending existing software (e.g., Sutherland and Royle 2019). Current applications of integrated models are simply the tip of the iceberg and will expand as technology and algorithm development continue (McClintock et al. 2021).

Acknowledgments

We thank Cat Sun and Angela Fuller for collecting the NY bears data. We thank Andy Royle for his contribution to the model development and the Sutherland Research Group for input. GD, DL, and CS conceptualized the study and integrated model. GD conducted simulations and analyses with input from DL and CS. GD wrote the manuscript with contributions from all authors.

Literature Cited

Bocinsky, R. K. 2016. FedData: functions to automate downloading geospatial data available from several federated data sources. R package version 2.0.4. https://doi.org/10.5281/zenodo.1306302

Borchers, D. L., and M. G. Efford. 2008. Spatially explicit maximum likelihood methods for capture–recapture studies. Biometrics 64:377–385.

Christ, A., J. Ver Hoef, and D. L. Zimmerman. 2008. An animal movement model incorporating home range and habitat selection. Environmental and Ecological Statistics 15:27–38.

Creel, S., J. Merkle, T. Mweetwa, M. S. Becker, H. Mwape, T. Simpamba, and C. Simukonda. 2020. Hidden Markov models reveal a clear human footprint on the movements of highly mobile African wild dogs. Scientific Reports 10:17908.

Crooks, K. R., C. L. Burdett, D. M. Theobald, S. R. King, M. Di Marco, C. Rondinini, and L. Boitani. 2017. Quantification of habitat fragmentation reveals extinction risk in terrestrial mammals. Proceedings of the National Academy of Sciences of the United States of America 114:7635–7640.

Crooks, K. R., C. L. Burdett, D. M. Theobald, C. Rondinini, and L. Boitani. 2011. Global patterns of fragmentation and connectivity of mammalian carnivore habitat. Philosophical Transactions of the Royal Society B: Biological Sciences 366:2642–2651.

Dijkstra, E. W., et al. 1959. A note on two problems in connexion with graphs. Numerische Mathematik 1:269–271.

Dupont, G., D. W. Linden, and C. Sutherland. 2021*a*. Supplement: Improved inferences about landscape connectivity from spatial capture-recapture by integration of a movement model. Open Science Framework. https://osf.io/684p9/

Dupont, G., J. A. Royle, M. A. Nawaz, and C. Sutherland. 2021*b*. Optimal sampling design for spatial capture–recapture. Ecology 102. https://doi.org/10.1002/ecy.3262.

Efford, M. 2004. Density estimation in live-trapping studies. Oikos 106:598–610.

Etten, J. V. 2017. R package gdistance: distances and routes on geographical grids. Journal of Statistical Software 76:1–21.

Gupta, A., B. Dilkina, D. J. Morin, A. K. Fuller, J. A. Royle, C. Sutherland, and C. P. Gomes. 2019. Reserve design to optimize functional connectivity and animal density. Conservation Biology 33:1023–1034.

Haddad, N. M., et al. 2015. Habitat fragmentation and its lasting impact on earth's ecosystems. Science Advances 1: e1500052.

Hanks, E. M., and M. B. Hooten. 2013. Circuit theory and model-based inference for landscape connectivity. Journal of the American Statistical Association 108:22–33.

Hooten, M. B., D. S. Johnson, B. T. McClintock, and J. M. Morales. 2017. Animal movement: statistical models for telemetry data. CRC Press, Boca Raton, Florida, USA.

Howell, P. E., E. Muths, B. R. Hossack, B. H. Sigafus, and R. B. Chandler. 2018. Increasing connectivity between metapopulation ecology and landscape ecology. Ecology 99:1119–1128.

Johnson, D. S., D. L. Thomas, J. M. Ver Hoef, and A. Christ. 2008. A general framework for the analysis of animal resource selection from telemetry data. Biometrics 64:968–976.

Levin, S. A. 1992. The problem of pattern and scale in ecology: the Robert H. MacArthur award lecture. Ecology 73:1943–1967.

Linden, D. W., A. P. Sirén, and P. J. Pekins. 2018. Integrating telemetry data into spatial capture–recapture modifies inferences on multi-scale resource selection. Ecosphere 9:e02203.

McClintock, B. T., B. Abrahms, R. Chandler, P. B. Conn, S. J. Converse, R. Emmet, B. Gardner, N. J. Hostetter, and D. S. Johnson. 2021. An integrated path for spatial capture-recapture and animal movement modeling. Ecology:e3473.

McRae, B. H., B. G. Dickson, T. H. Keitt, and V. B. Shah. 2008. Using circuit theory to model connectivity in ecology, evolution, and conservation. Ecology 89:2712–2724.

Moorcroft, P. R., and A. Barnett. 2008. Mechanistic home range models and resource selection analysis: a reconciliation and unification. Ecology 89:1112–1119.

Morales, J. M., P. R. Moorcroft, J. Matthiopoulos, J. L. Frair, J. G. Kie, R. A. Powell, E. H. Merrill, and D. T. Haydon. 2010. Building the bridge between animal movement and population dynamics. Philosophical Transactions of the Royal Society B: Biological Sciences 365:2289–2301.

Morin, D. J., A. K. Fuller, J. A. Royle, and C. Sutherland. 2017. Model-based estimators of density and connectivity to inform conservation of spatially structured populations. Ecosphere 8:e01623.

Murphy, S. M., D. T. Wilckens, B. C. Augustine, M. A. Peyton, and G. C. Harper. 2019. Improving estimation of puma (puma concolor) population density: clustered camera-trapping, telemetry data, and generalized spatial mark-resight models. Scientific Reports 9:1–13.

Plard, F., R. Fay, M. Kéry, A. Cohas, and M. Schaub. 2019. Integrated population models: powerful methods to embed individual processes in population dynamics models. Ecology 100:e02715.

R Core Team. 2020. R: a language and environment for statistical computing. R Foundation for Statistical Computing, Vienna, Austria. https://www.r-project.org/

Rayfield, B., M.-J. Fortin, and A. Fall. 2011. Connectivity for conservation: a framework to classify network measures. Ecology 92:847–858.

Revilla, E., and T. Wiegand. 2008. Individual movement behavior, matrix heterogeneity, and the dynamics of spatially structured populations. Proceedings of the National Academy of Sciences of the United States of America 105:19120–19125.

Royle, J. A., R. B. Chandler, K. D. Gazenski, and T. A. Graves. 2013*a*. Spatial capture–recapture models for jointly estimating population density and landscape connectivity. Ecology 94:287–294.

Royle, J. A., R. B. Chandler, R. Sollmann, and B. Gardner. 2013*b*. Spatial capture-recapture. Academic Press, Cambridge, Massachusetts, USA.

Royle, J. A., R. B. Chandler, C. C. Sun, and A. K. Fuller. 2013*c*. Integrating resource selection information with spatial capture–recapture. Methods in Ecology and Evolution 4:520–530.

Royle, J. A., A. K. Fuller, and C. Sutherland. 2018. Unifying population and landscape ecology with spatial capture–recapture. Ecography 41:444–456.

Royle, J. A., and K. V. Young. 2008. A hierarchical model for spatial capture–recapture data. Ecology 89:2281–2289.

Sciaini, M., M. Fritsch, C. Scherer, and C. E. Simpkins. 2018. Nlmr and landscapetools: An integrated environment for simulating and modifying neutral landscape models in r. Methods in Ecology and Evolution 9:2240–2248.

Shaw, A. K. 2020. Causes and consequences of individual variation in animal movement. Movement Ecology 8:1–12.

Sollmann, R., B. Gardner, J. L. Belant, C. M. Wilton, and J. Beringer. 2016. Habitat associations in a recolonizing, low-density black bear population. Ecosphere 7:e01406.

Sollmann, R., B. Gardner, A. W. Parsons, J. J. Stocking, B. T. McClintock, T. R. Simons, K. H. Pollock, and A. F. O'Connell. 2013. A spatial mark–resight model augmented with telemetry data. Ecology 94:553–559.

Spiegel, O., S. T. Leu, C. M. Bull, and A. Sih. 2017. What's your move? Movement as a link between personality and spatial dynamics in animal populations. Ecology Letters 20:3–18.

Sun, C. 2014. Estimating black bear population density in the southern black bear range of New York with a non-invasive, genetic, spatial capture-recapture study. Thesis. Cornell University.

Sutherland, C., A. K. Fuller, and J. A. Royle. 2015. Modelling non-Euclidean movement and landscape connectivity in highly structured ecological networks. Methods in Ecology and Evolution 6:169–177.

Sutherland, C., J. A. Royle, and D. W. Linden. 2019. oscr: A spatial capture–recapture r package for inference about spatial ecological processes. Ecography 42:1459–1469.

Tenan, S., P. Pedrini, N. Bragalanti, C. Groff, and C. Sutherland. 2017. Data integration for inference about spatial processes: A model-based approach to test and account for data inconsistency. PLOS ONE 12:e0185588.

Tischendorf, L., and L. Fahrig. 2000. How should we measure landscape connectivity? Landscape Ecology 15:633–641.

Tischendorf, L., A. Grez, T. Zaviezo, and L. Fahrig. 2005. Mechanisms affecting population density in fragmented habitat. Ecology and Society 10:1–13.

Yang, L., et al. 2018. A new generation of the United States national land cover database: Requirements, research priorities, design, and implementation strategies. ISPRS Journal of Photogrammetry and Remote Sensing 146:108–123.

Zeller, K. A., K. McGarigal, and A. R. Whiteley. 2012. Estimating landscape resistance to movement: a review. Landscape Ecology 27:777–797.

Supporting Information

Additional supporting information may be found in the online version of this article at http://onlinelibrary.wiley.com/doi/10.1002/ecy.3544/suppinfo

Open Research

Code (Dupont et al. 2021) is archived at the Open Science Framework repository: https://doi.org/10.17605/OSF.IO/684P9